XMAP215 polymerase activity is built by combining multiple tubulin-binding TOG domains and a basic lattice-binding region

Per O. Widlund[a], Jeffrey H. Stear[b], Andrei Pozniakovsky[a], Marija Zanic[a], Simone Reber[a], Gary J. Brouhard[c], Anthony A. Hyman[a,1], and Jonathon Howard[a,1]

[a]Max Planck Institute of Molecular Cell Biology and Genetics, Pfotenhauerstrasse 108, 01307 Dresden, Germany; [b]Institut für Biologie, Humboldt Universität zu Berlin, Chausseestrasse 117, 10115 Berlin, Germany; and [c]Department of Biology, McGill University, 1205 avenue Docteur Penfield, Montréal, QC, Canada H3A 1B1

Edited by J. Richard McIntosh, University of Colorado, Boulder, CO, and approved December 30, 2010 (received for review November 3, 2010)

XMAP215/Dis1 family proteins positively regulate microtubule growth. Repeats at their N termini, called TOG domains, are important for this function. While TOG domains directly bind tubulin dimers, it is unclear how this interaction translates to polymerase activity. Understanding the functional roles of TOG domains is further complicated by the fact that the number of these domains present in the proteins of different species varies. Here, we take advantage of a recent crystal structure of the third TOG domain from *Caenorhabditis elegans*, Zyg9, and mutate key residues in each TOG domain of XMAP215 that are predicted to be important for interaction with the tubulin heterodimer. We determined the contributions of the individual TOG domains to microtubule growth. We show that the TOG domains are absolutely required to bind free tubulin and that the domains differentially contribute to XMAP215's overall affinity for free tubulin. The mutants' overall affinity for free tubulin correlates well with polymerase activity. Furthermore, we demonstrate that an additional basic region is important for targeting to the microtubule lattice and is critical for XMAP215 to function at physiological concentrations. Using this information, we have engineered a "bonsai" protein, with two TOG domains and a basic region, that has almost full polymerase activity.

Cells assemble and disassemble actin filaments and microtubules to carry out a vast array of functions, such as defining cell shape, directing cellular movement, and mediating chromosome segregation and cell division. Although these polymeric filaments have different structures and display different dynamics, the cell regulates their assembly and disassembly in related ways. Polymer growth is polar in both cases and occurs at the plus ends of microtubules and the barbed ends of actin filaments. Both polymers have specific nucleating proteins, assemble with the help of polymerases, and disassemble with the aid of severing proteins and depolymerases (1–4). How these various activities coordinate to create the cytoskeleton is a central question in cell biology (5). This work focuses on assembly.

The main promoters of polymer growth are the XMAP215/Dis family for microtubules and the formins for actin (4, 6–9). The function of formins in actin polymerization is well characterized. Formins have two key domains that are important for their activity, FH1 and FH2 (8, 10). While the FH2 domain is necessary for binding to the barbed end of actin, repeats of polyproline in the FH1 domain are required to interact with actin/profilin complexes and recruit them to the barbed end (4, 11, 12).

Much less is known about how the regions of XMAP215 coordinate in promoting microtubule growth (13). Recent work has shown that XMAP215 acts as a classic catalyst (14). At physiological tubulin concentrations, XMAP215 is a tubulin polymerase that promotes incorporation of tubulin into the growing plus end. However, in the absence of free tubulin, XMAP215 accelerates depolymerization of GMPCPP-stabilized microtubules. Therefore, XMAP215 can act both as a polymerase and a depolymerase, and its activity depends on the concentration of its substrate, tubulin. However, how the various domains of the XMAP215 protein contribute to these activities is not known.

Members of the XMAP215/Dis1 family are characterized by a varying number of TOG domains at their N termini (Fig. 1). Based on mutants in TOG domains that interfere with tubulin binding (15) and protein activity (16–20), it has been proposed that TOG binding to tubulin is required for its catalytic activity (21); however, there is no proof for this idea. It is also not known how the various properties of XMAP215—association with the tubulin dimer, binding to the microtubule lattice and plus end, diffusion along the lattice—depend on the TOG domains. We have therefore sought to determine how the TOG domains, and possibly other domains, contribute to microtubule polymerase activity.

Results

TOG Domains are Required to Bind Free Tubulin and for Microtubule Polymerization. Two key loops in TOG3 of Zyg9, the XMAP215/Dis1 homolog in *Caenorhabditis elegans*, were previously identified as being important for interaction with free tubulin (15). We mutated two conserved residues in the corresponding conserved loops of all five TOG domains of XMAP215 to determine their contribution to microtubule growth promotion (Fig. 1). This TOG1-5AA mutant did not promote growth under any conditions (Fig. 2*A*). We assayed for growth above 5 μM tubulin because no growth is seen at or below this concentration in the absence of any growth-promoting factor due to the high frequency of catastrophes at low tubulin concentrations (14). We then assayed this mutant for the other properties characteristic of the wild-type protein: free tubulin binding, microtubule binding, microtubule lattice diffusion, and tip tracking. The mutant's affinity for free tubulin was severely reduced, as shown by size exclusion chromatography (Fig. 2*B* and *C*).

TOGs 1 and 2 are Critical for Polymerase Activity. These data demonstrate that the TOG domains play an essential function in mediating XMAP215's ability to bind free tubulin and in promoting microtubule growth; however, they do not allow us to assess the contribution of individual TOG domains. To address this question, we generated a series of constructs in which TOG domains

Author contributions: P.O.W., J.H.S., A.P., G.J.B., A.A.H., and J.H. designed research; P.O.W., J.H.S., A.P., and S.R. performed research; P.O.W., J.H.S., M.Z., G.J.B., A.A.H., and J.H. analyzed data; and P.O.W., J.H.S., M.Z., A.A.H., and J.H. wrote the paper.

The authors declare no conflict of interest.

This article is a PNAS Direct Submission.

Freely available online through the PNAS open access option.

[1]To whom correspondence may be addressed. E-mail: hyman@mpi-cbg.de or howard@mpi-cbg.de.

This article contains supporting information online at www.pnas.org/lookup/suppl/doi:10.1073/pnas.1016498108/-/DCSupplemental.

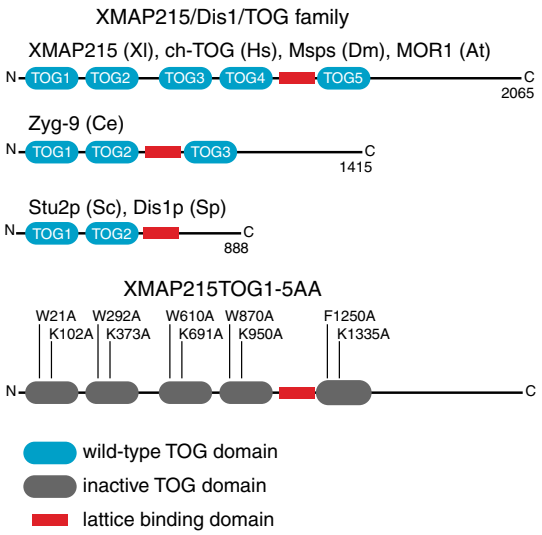

Fig. 1. XMAP215 and its homologues. (*A*) The three major classes of TOG proteins. The human, frog, fly, plant, worm, and yeast homologues are shown. (*B*) Positions of the point mutations in XMAP215TOG1-5AA.

were individually or pair-wise mutated. We tested the ability of these combinations of TOG mutants to promote microtubule growth using two different assays. First, we determined the activities of the various mutants at a fixed tubulin concentration of 5 μM. No growth was seen from microtubule seeds with 5 μM tubulin alone (as noted above). However, when full length XMAP215 was added, we saw a dose dependent increase in growth rate that reached a maximum at approximately 200 nM protein. All functional point mutants reached maximum growth at this concentration but with significantly different maximum growth rates (V_{max}) (Fig. 3*A*). And second, we measured the microtubule growth rate over a range of tubulin concentrations at a fixed XMAP215 concentration of 200 nM. The growth rates increased linearly with tubulin concentration for all mutants; however, the mutants displayed a strikingly different contribution to polymerization activity (Fig. 3*B*). The two assays gave consistent results: The mutation of TOGs 3/4 and TOG 5 had marginal effects on activity. TOG 1 and TOG 2 contributed strongly to the activity; and the double mutation of TOG 1 and 2 resulted in a protein with minimal polymerase activity.

Polymerase Activity Correlates with Binding to Free Tubulin Dimers. Considering that mutation of all TOG domains in the full length protein prevented interaction with free tubulin dimers, we wanted to see how competent our array of mutants were to bind free tubulin. As was done for the wild-type GFP-tagged protein, we determined this by size exclusion chromatography. As a measure of tubulin binding, we computed amount of tubulin bound per XMAP215 (Figs. S1 and S2). In order to compare tubulin binding to growth, we determined the V_{max} for all mutants by repeating the growth experiments at saturating XMAP215 concentrations (200 and 400 nM). Their abilities to bind tubulin fell in a range between that of the wild-type protein and the TOG1-5AA mutant (Fig. S1). In fact, the amount of tubulin bound per XMAP215 was proportional to the polymerase activity (Fig. 3*C*). Therefore, all TOG domains contribute to both the affinity of XMAP215 for the tubulin dimer and polymerization activity, suggesting that the affinity for tubulin plays an important role in the polymerization mechanism (see *Discussion*).

Efficiency of Polymerase Activity Increases with Increasing Lattice Affinity. Since TOGs 1 and 2 showed the most significant contribution to activity, we asked whether they were sufficient to promote microtubule growth. We expressed an XMAP215 fragment

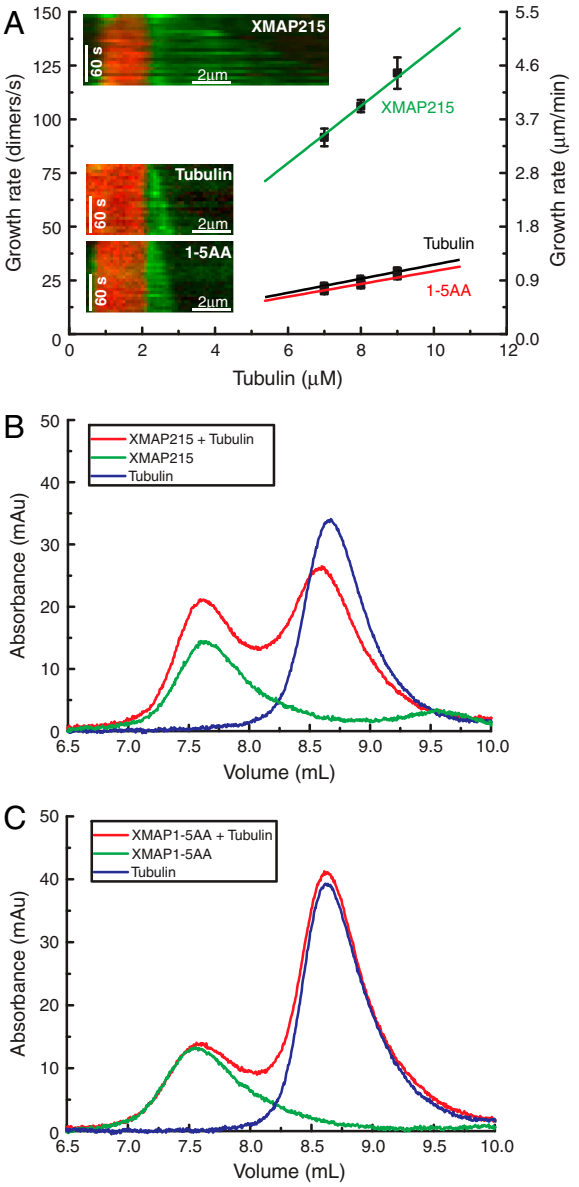

Fig. 2. XMAP215TOG1-5AA-GFP does not promote microtubule growth and does not bind tubulin. (*A*) XMAP215-GFP shows a fivefold increase in tubulin growth at all tubulin concentrations examined while XMAP215-TOG1-5AA-GFP does not. Error bars represent SEM ($N \geq 15$ for each point). Kymographs show a representative single microtubule from each experiment. Trend lines project back to the critical concentration in the absence of catastrophes. Rhodamine-labeled GMPCPP seeds are in red. Alexa488 labeled tubulin is in green. (*B*) XMAP215-GFP binds tubulin. Chromatography experiments showing A280 over elution volume. Three traces are shown in each graph: XMAP215-GFP alone in green, tubulin alone in blue, XMAP215-GFP in combination with tubulin in red. (*C*) XMAP215TOG1-5AA-GFP does not bind tubulin. Chromatography experiments showing A280 over elution volume. Three traces are shown in each graph: XMAP215TOG1-5AA-GFP alone in green, tubulin alone in blue, XMAP215-GFP in combination with tubulin in red.

containing just TOGs 1 and 2 in *Escherichia coli*. This fragment had little polymerase activity at 200 nM protein, where we see maximal growth with wild-type protein (Fig. 3*A*). We therefore attempted to determine what features displayed by the wild-type protein were absent with the TOG12 fragment. The TOG12 fragment was still able to bind tubulin dimers (Fig. 4*A*) and microtubule ends (Fig. 4*D*); however, it had a severely reduced affinity for the microtubule lattice (Fig. 4*B*). We therefore tested whether addition of a microtubule-binding domain would enhance the

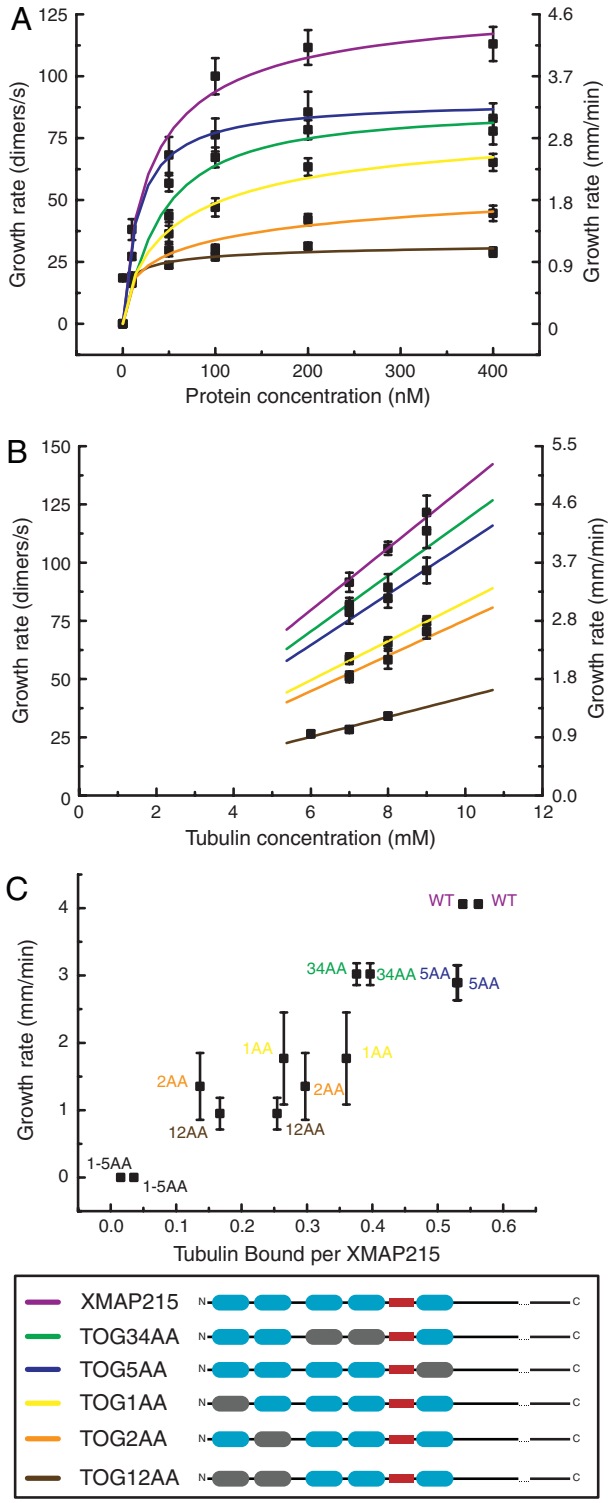

Fig. 3. Characterization of all XMAP215 TOG domain point mutants. (*A*) Microtubule growth rate by XMAP215-GFP and all point mutants with increasing XMAP215 concentration at 5 μM tubulin. Error bars represent SEM ($N \geq 10$ for each point). (*B*) Growth promotion by XMAP215-GFP and all point mutants with increasing tubulin concentration. Error bars represent SEM ($N \geq 10$ for each point). (*C*) Maximum average growth rate of individual XMAP215 mutants plotted against their ability to bind tubulin as determined from chromatograms (Figs. S1 and S2). The maximum average growth rate was determined in at least four separate experiments at either 200 or 400 nM protein. Because no significant difference was seen between 200 and 400 nM protein for each construct, the rates were averaged ($N \geq 10$ for each experiment). Error bars represent SEM. Tubulin binding was measured in duplicate.

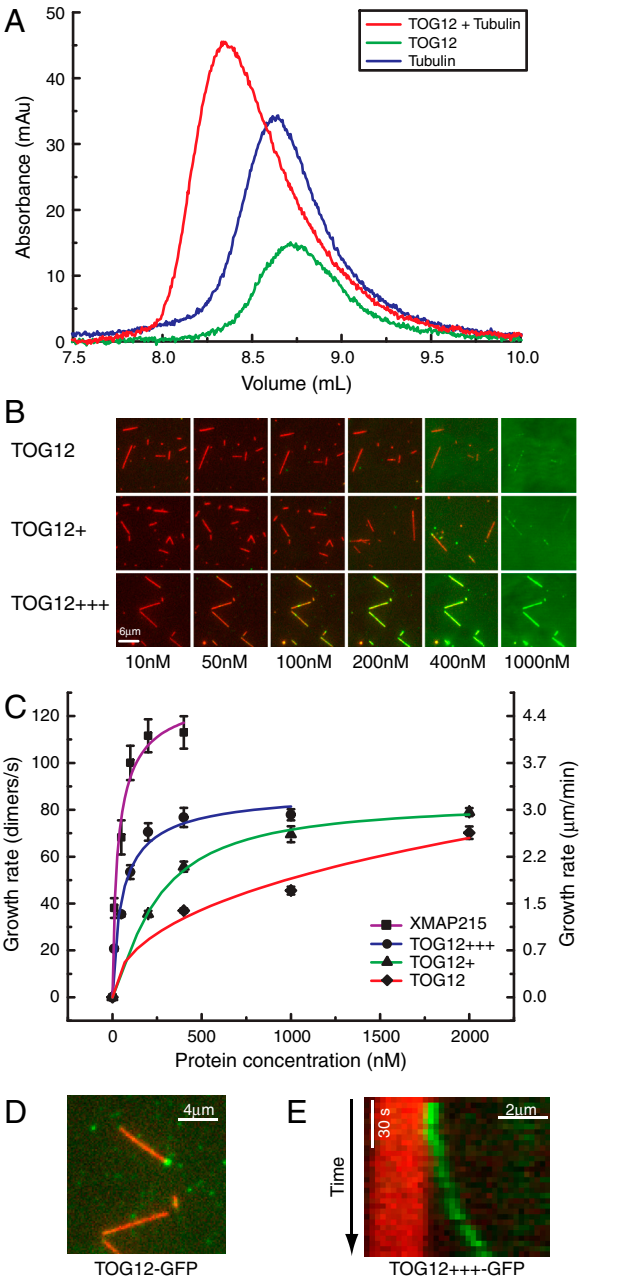

Fig. 4. Construction of a minimal polymerase. (*A*) TOG12 binds tubulin. Chromatography experiments showing A280 over elution volume. Three traces are shown in each graph: TOG12 alone in green, tubulin alone in blue, TOG12 in combination with tubulin in red. (*B*) The Kif2A lattice-binding domain increases affinity of TOG12 for the microtubule lattice. Fragments were incubated with rhodamine-labeled GMPCPP-stabilized microtubules with increasing protein concentration as indicated. The merged image shows microtubules in red and GFP in green. (*C*) Microtubule growth rate with increasing TOG12, TOG12+, and TOG12+++ concentration at 5 μM tubulin. Error bars represent SD ($N \geq 10$ for each point). (*D*) TOG12 binds the plus end of stabilized GMPCPP seeds. Rhodamine-labeled GMPCPP seeds are in red. TOG12-GFP is in green. (*E*) TOG12+++ GFP tracks growing microtubule plus ends. Rhodamine-labeled GMPCPP seeds are in red. TOG12+++GFP is in green.

activity of the TOG12 fragment at lower concentrations. We decided to use the K-loop of the kinesin KIF1A to target the TOG12 fragment to the microtubule lattice. We chose this loop because it is a simple basic region that has been reported to effectively target KIF1A and another kinesin, MCAK, to the microtubule lattice (22, 23), and we wanted to exclude other

activities that were potentially present in the region surrounding the native microtubule-lattice-binding domain. Indeed, addition of one K-loop increased the affinity of the TOG12 fragment to the microtubule lattice; addition of three repeats of this domain further increased microtubule-binding activity (Fig. 4*B*), similar to that of the wild-type protein (see below). We then assayed the ability of these fusion proteins to promote microtubule growth. While the TOG12 fragment alone showed activity at or above 400 nM protein, the TOG12+ and TOG12+++ were active at much lower concentrations. Strikingly, all fragments appear to have a maximum growth rate of approximately 3 μm/min but reach this maximum at very different protein concentrations (Fig. 4*C*). Furthermore, their activities correspond very well with the fragments' affinities for the microtubule lattice. These experiments define a minimal "bonsai" polymerase, namely a TOG12 fragment with a strong microtubule-binding domain, which behaves very similar to the wild-type protein. It binds tubulin and the microtubule lattice, promotes fast growth in the low nM range, and is able to track growing microtubule tips (Fig. 4*E* and Movie S1).

The XMAP215 Microtubule-Lattice-Binding Domain Lies Between TOG4 and TOG5. Because the TOG12 fragment depended on a microtubule-lattice-binding domain to function, we suspected that the native XMAP215 has a microtubule-lattice-binding domain. A region with high affinity (K_D < 1 μM) for microtubules was mapped to a region between residues 1150 and 1325 (13, 24). This region includes part of a region between TOG4 and TOG5 as well as part of TOG5 itself. We wanted to know if TOG5 or any of the TOGs are involved in lattice binding. A fragment containing TOG1-4 (residues 1–1081) bound poorly to the microtubule lattice, consistent with published observations (Figure 5). We made an additional fragment containing the region up to TOG5 (residues 1–1235); it bound microtubules similar to wild type (Fig. 5). Taken together with the published analyses, our experiments suggest that the microtubule-binding domain resides in the region between residues 1150 and 1235, a region that excludes TOG5.

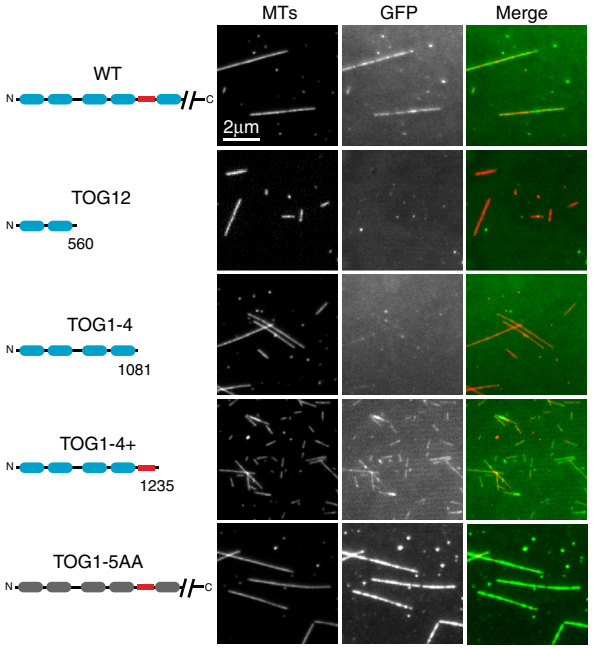

Fig. 5. The microtubule-lattice-binding domain lies between TOG4 and TOG5. 200 nM XMAP215-GFP and various deletion mutants were incubated with rhodamine-labeled GMPCPP-stabilized microtubules and imaged. The left image shows the microtubules. The center image shows the GFP signal. The right image shows the merged image with microtubules in red and GFP in green.

This region is basic, with a predicted pI of 9.8. This is consistent with what is seen in XMAP215 homologues. The *Saccharomyces cerevisiae* homologue of XMAP215, Stu2, has a basic linker after the TOG domains, which has been shown to bind to the microtubule lattice (17, 21). This basic region is also found in *Schizosaccharomyces pombe* Dis1 (25). This region combined with the TOG domains cooperate to promote robust microtubule growth at nanomolar concentrations of protein.

Discussion

We have shown that the ability of XMAP215 to efficiently catalyze the incorporation of tubulin dimers into a microtubule is dependent on tubulin binding and microtubule-lattice-binding. We further demonstrate that these activities are mediated by functionally distinct domains. Multiple TOG domains are necessary to increase affinity for the tubulin dimer. Mutants in which these interactions are disrupted are able to efficiently target the microtubule lattice but are impaired in their capacity to promote the incorporation of tubulin dimers into a growing microtubule end. We have also identified a microtubule-lattice-binding domain on XMAP215, localized between TOGs 4 and 5. Deletion of this basic region strongly inhibits the association of XMAP215 with the microtubule lattice. However, protein fragments lacking this domain are still able to promote robust microtubule growth when artificially targeted to the microtubule lattice.

The microtubule plus end can be thought of as an enzyme for the incorporation of tubulin. This enzyme is inefficient, however, because the growth rate in pure tubulin is well below the diffusion limit: The association rate of GTP-tubulin for the individual protofilament plus ends is only 0.3 $\mu M^{-1}\,s^{-1}$, about 20 times smaller than that of ATP-actin for individual protofilament barbed ends in an actin filament (26). It is likely that only a fraction of the tubulin dimers that collide with the plus end become stably incorporated into the microtubule lattice. XMAP215 can be thought of as a nonessential activator of the microtubule end that increases the fraction of tubulin dimers that successfully incorporate into the microtubule lattice (14, 27). When sufficient XMAP215 is added to saturate the plus end, the association rate is increased fivefold to 1.5 $\mu M^{-1}\,s^{-1}$ (per protofilament plus end).

In this work, we demonstrate that removal of functional TOG domains affects the ability of XMAP215 to increase the association rate for tubulin to the microtubule plus end. Accordingly, all of the TOG domain point mutants we described showed a lowered maximal growth rate as well as an association rate that falls between 0.3 and 1.5 $\mu M^{-1}\,s^{-1}$ per protofilament end. At a fixed tubulin concentration, addition of increasing amounts of XMAP215 resulted in a dose response that achieved maximal growth rate at approximately 200 nM protein, suggesting that the plus ends are saturated with XMAP215 at this concentration. All of the point mutants reached their maximal growth rate at approximately 200 nM protein, consistent with the idea that these proteins are able to bind to the microtubule lattice and target to the plus end similar to the wild-type protein. We therefore conclude that the TOG domains and the tubulin affinity they confer determine the maximal growth rate (ν_{max}) at any fixed tubulin concentration and the decreased capacity for promoting microtubule growth observed with these mutants can be attributed to the fact that ends are saturated with a less effective polymerase (Fig. 6*A*).

XMAP215 requires a region between TOGs 4 and 5 to target to the microtubule lattice. This positively charged linker may bind to the E-hooks of microtubules, because it has been shown that XMAP215 binds poorly to microtubules whose E-hooks have been removed by subtilisin treatment (14). Removal of the microtubule-binding domain affects the ability of the TOG domains of XMAP215 to work at lower concentrations. The processivity of XMAP215 at the microtubule plus end can be attributed to a combination of tubulin binding and incorporation into the lattice followed by lattice diffusion to the new end via the interaction

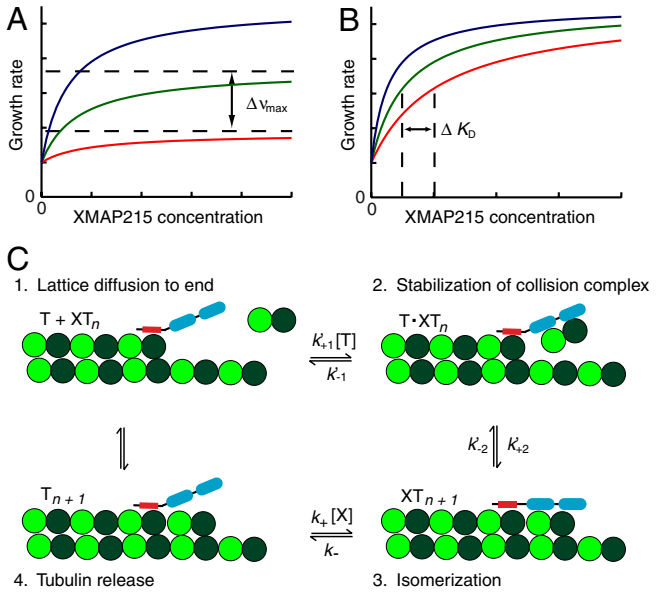

Fig. 6. XMAP215 as a catalyst. (*A*) Mutation or removal of TOG domains result in mutants that have lowered maximal growth rates (ν_{max}) at any fixed tubulin concentration. The graph shows theoretical dose response of a protein with increasing affinities for the tubulin dimer that lead to increasing affinities for the transition state (compared to the microtubule end alone): $\alpha = 2$ in red, $\alpha = 5$ in green, and $\alpha = 10$ in blue. $\beta = 1$, $[T] = 0.1K_1$ (see *SI Text*). (*B*) Mutation or removal of the microtubule-binding domain in XMAP215 results in constructs that have the same ν_{max} but a higher K_D. The graph shows theoretical dose response of a protein with a constant ν_{max} and an altered k_{on} for microtubule-lattice binding: 4x reduced in red, 2x reduced in green, not reduced in blue. $\beta = 1$, $[T] = 0.1K_1$ (see *SI Text*). (*C*) Model of TOG12+++ on the plus end of a microtubule. (1) Diffusion to the end via the lattice-binding domain. (2) TOG12+++ stabilizes the incoming dimer. (3) TOG12+++ remains bound to the incorporated dimer. (4) Release of the dimer. The transitions between each state are described by the reaction scheme in the *SI Text*.

between the lattice-binding domain and the E-hooks. We showed that a TOG12 construct became effective at lower concentrations when the affinity for the microtubule lattice was increased by the addition of a nonnative microtubule-binding domain. TOG12 is still able to bind and diffuse along the microtubule lattice without this domain and can even bind the microtubule plus end at low nanomolar concentrations but needs to be at a much higher concentration in solution to saturate the growing plus end. As microtubule-lattice-binding domains are added to this fragment, its affinity for the microtubule is increased resulting in a higher flux of XMAP215 to the growing plus end (Fig. 6*B*). A consequence of increased flux is that plus ends become saturated at lower concentrations of protein in solution. We propose that XMAP215 and the TOG12+++ fragment target to and maintain association with the growing plus end by a mechanism that is similar to their association with the microtubule lattice, namely through basic regions. Once targeted to the end, the tubulin affinity determines the maximal growth rate (ν_{max}) at any fixed tubulin concentration (Fig. 6*A*).

The TOG12+++ bonsai protein displayed characteristics very similar to wild-type XMAP215. We therefore define this as a minimal polymerase. It binds and diffuses on the microtubule lattice, tracks polymerizing and depolymerizing plus ends, binds tubulin, and promotes growth exclusively at the plus end. The maximal growth rate was 3 μm/min at 5 μM tubulin as opposed to 4 μm/min for wild-type XMAP215. The absence of TOGs 3, 4, and 5 can account for this difference as mutation of these TOGs resulted in mutants that showed similar maximal growth rates. The K_D for this construct was also slightly higher compared to wild-type due to differences in affinities of the nonnative and native microtubule-lattice-binding domains.

Because the nondimerized TOG12 is sufficient to promote robust microtubule growth, we consider this further evidence against growth promotion by addition of oligomers to the microtubule plus end (19, 28, 29). TOG12 could bind at most an oligomer of 2 dimers but not 5–7 dimers as required by a shuttle model. Instead, we argue that the additional TOG domains provide additional affinity for individual tubulin dimers. To be a catalyst, XMAP215 must bind tubulin with a high affinity but also be able to release once the tubulin has been incorporated. Therefore, multiple binding sites within the same molecule that have high off rates would be ideal. The combined avidity of the multiple TOG domains results in strong overall binding, while the high off rates of individual TOG domains could allow for quick release.

As with the formins in actin polymerization, we have now separated domains that are critical for XMAP215 function. Formins have FH1 and FH2 domains, whereas XMAP215 has TOG domains and a basic lattice-binding region. There are, however, some notable differences. While formins use polyproline repeats in FH1 domains to recruit multiple G-actin monomers, TOG domains are used to increase affinity for one tubulin dimer. Furthermore, while FH2 domains link formins to the barbed end, the basic lattice-binding domain does not bind the end specifically. Instead, TOG domains are critical for catalysis while the basic lattice-binding domain is important for targeting to the microtubule end. We propose that the processive polymerization of XMAP215 is a combination of tubulin binding from solution and incorporation into the lattice, followed by lattice diffusion to the new end via the interaction between the lattice-binding domain and the E-hooks (Fig. 6*C*). The TOG12 fragment with low lattice-binding activity can still associate specifically with the ends of GMPCPP-stabilized microtubules (Fig. 4*D*), suggesting that the TOG domains recognize a surface that is not exposed on the microtubule lattice. We found that none of our mutants separated microtubule end binding and tip-tracking activity from tubulin binding, suggesting that those contacts that are made to free tubulin are the same as those made to tubulin that has newly been incorporated into the microtubule lattice. Therefore, consistent with the idea that XMAP215 is a catalyst (14), TOG domains bind to free tubulin, incorporated tubulin, and the transition state between the two in a similar way. We propose that it is the affinity for this transition state that determines the maximal growth rate (ν_{max}) at a fixed tubulin concentration. Furthermore, our observation that the growth rate at any XMAP215 protein concentration correlates with the affinity of that protein for the microtubule lattice implies that XMAP215 associates with the microtubule end in a similar way that it binds to the microtubule lattice. Thus, the presumed electrostatic interaction with the lattice also occurs at the ends. We have incorporated these data into the previous kinetic model (see *SI Text*).

Materials and Methods

Plasmid Construction. A pFastBac construct with XMAP215-GFP was described previously (14). A fragment containing all five TOGs with the following mutations was synthesized: W21A, K102A, W292A, K373A, W610A, K691A, W870A, K950A, F1250A, K1335A. This EcoRI, KasI fragment was cloned into the XMAP215-GFP vector to give XMAP215-TOG1-5AA-GFP. Subsequent combinations of TOG mutations were made by switching TOGs between plasmids using unique restriction sites between them: StuI, NotI, AatII, AgeI. TOG1-4GFP, TOG1-4+GFP, ΔTOG1-4GFP, and ΔTOG1-4+GFP were made by amplifying a PCR fragment lacking the region to be deleted, followed DpnI digestion and subsequent ligation of the blunt ended fragment (linear plasmid) to circularize the plasmid. TOG12 is the same as fragment 1 described in ref. 16. All remaining fragments were derived from this plasmid by mutagenesis described above. The TOG12 "bonsai" construct (30) was made by inserting the following sequence into a SalI site a the 3′ end: tcgacaataagaacaaaaagaaaaagaaagtcgacaataagaacaaaaagaaaaagaaagtcgac.

The GFP tag was introduced on a NotI fragment into the 3′ end after the microtubule-binding domain.

Protein Expression and Purification. Full length XMAP215, XMAP215-GFP, all full length point mutants, TOG1-4GFP, TOG1-4+GFP, ΔTOG1-4GFP, and ΔTOG1-4+GFP were expressed in SF+ cells using the Bac-to-Bac system from Invitrogen essentially as described previously (14) except baculovirus infected insect cell (BIIC) stocks were used (31) (see *SI Text*). All remaining constructs were expressed in *E. coli* BL21 with plasmid pRARE (see *SI Text*).

Tubulin and Microtubule Preparation. Porcine brain tubulin was purified as described (32). Labeling of cycled tubulin with Alexa Fluor 488 or TAMRA (Invitrogen) was performed as described (33). GMPCPP microtubules were grown as described (34).

Imaging. The total-internal-reflection fluorescence imaging was performed with a setup described previously (14, 34, 35). The setup incorporates an Andor DV887 iXon camera on a Zeiss Axiovert 200 M microscope using a Zeiss 100X/1.45 a Plan-FLUAR objective. Standard filter sets were used to visualize tetramethylrhodamine, Alexafluor 488, and GFP.

Assay Conditions. The preparation of silanized cover glasses and perfusion chambers was previously described (14, 34, 35). Reaction channels were first rinsed with BRB80: 80 mM PIPES at pH 6.9, 1 mM MgCl2, and 1 mM EGTA. Reaction channels were incubated with either 1% antirhodamine antibody (Invitrogen) or 50 μg/mL neutravidin (Sigma) in BRB80 for 5 min, followed by 1% pluronic F127 (Sigma) in BRB80 for 5 min, and finally rhodamine-labeled or rhodamine and biotinylated, GMPCPP-stabilized microtubule seeds for 15 min. Channels were washed once with BRB80 and once with imaging buffer (IB): BRB80 supplemented with 75 mM KCl, 0.1 mg/ml BSA, 1% β-mercaptoethanol, 40 mM glucose, 40 mg/ml glucose oxidase, and 16 mg/ml catalase. We used an objective heater (Zeiss) to warm the sample to 35 °C. Microtubule growth at a fixed tubulin concentration and increasing XMAP215 concentration was done with 4.5 μM unlabeled tubulin, 0.5 μM Alexa Fluor 488 tubulin, XMAP215-GFP (0–200 nM), and 1 mM GTP. Microtubule growth with increasing tubulin concentration and fixed XMAP215 concentration was done with 6, 7, 8 or 7, 8, and 9 μM tubulin by combining varying amounts of 6 μM tubulin (5.5 μM unlabeled tubulin, 0.5 μM Alexa Fluor 488 tubulin) and 9 μM tubulin (8 μM unlabled, 1.0 μM Alexa Fluor 488 tubulin), 200 nM XMAP215, and 1 mM GTP.

Size Exclusion Chromatography. Size exclusion chromatography was carried out similar to ref. 14. Briefly, a Tosoh TSKgelG5000PWXL column was equilibrated in 25 mM TrisHCl pH 7.5, 75 mM NaCl, 1 mM MgCl2, 1 mM EGTA, 0.1% Tween20, 1 mM DTT. XMAP215 (5.7 μM) and tubulin (14.7 μM) or the equivalent buffer in case of single protein injection were mixed with 0.2 mM GTP in 50 μL total volume, incubated for 10 min on ice and then injected onto the Tosoh TSKgelG5000PWXL size exclusion column. For the TOG12 binding experiment, 15 μM TOG12 and 15 μM tubulin were used in 50 μL total volume.

Data Analysis. Microtubule growth measurements were performed in Metamorph (Universal Imaging). Images were processed using Metamorph and Image J. Curve fitting was done in OriginPro (Origin Lab). Tubulin binding was determined using the heights of the XMAP215, XMAP215:Tubulin and Tubulin peaks (Fig. S2).

ACKNOWLEDGMENTS. We thank J. Al-Bassam and S. Harrison for helpful discussions; D. Drechsel, B. Borgonovo, and R. Lemaitre for advice and technical assistance; and C. Gell for help with microscopy. We thank members of the Hyman and Howard laboratories for advice and discussions. P.O.W. was supported by a European Molecular Biology Organization long-term fellowship, J.H.S. was supported by the National Institutes of Health National Research Service Award program and the Deutsche Forschungsgemeinschaft, G.J.B. acknowledges support from the Natural Sciences and Engineering Research Council of Canada (Grant 372593). M.Z. is supported by the International Human Frontier Science Program Organization. This work was funded by the Max Planck Society.

1. Howard J, Hyman AA (2007) Microtubule polymerases and depolymerases. *Curr Opin Cell Biol* 19:31–35.
2. Pantaloni D, Le Clainche C, Carlier MF (2001) Mechanism of actin-based motility. *Science* 292:1502–1506.
3. Desai A, Mitchison TJ (1997) Microtubule polymerization dynamics. *Annu Rev Cell Dev Biol* 13:83–117.
4. Paul A, Pollard T (2009) Review of the mechanism of processive actin filament elongation by formins. *Cell Motil Cytoskeleton* 66:606–617.
5. Goode BL, Drubin DG, Barnes G (2000) Functional cooperation between the microtubule and actin cytoskeletons. *Curr Opin Cell Biol* 12:63–71.
6. Gard DL, Kirschner MW (1987) A microtubule-associated protein from Xenopus eggs that specifically promotes assembly at the plus-end. *J Cell Biol* 105:2203–2215.
7. Gard DL, Kirschner MW (1987) Microtubule assembly in cytoplasmic extracts of Xenopus oocytes and eggs. *J Cell Biol* 105:2191–2201.
8. Goode BL, Eck MJ (2007) Mechanism and function of formins in the control of actin assembly. *Annu Rev Biochem* 76:593–627.
9. Kinoshita K, Habermann B, Hyman AA (2002) XMAP215: A key component of the dynamic microtubule cytoskeleton. *Trends Cell Biol* 12:267–273.
10. Sagot I, Rodal AA, Moseley J, Goode BL, Pellman D (2002) An actin nucleation mechanism mediated by Bni1 and profilin. *Nat Cell Biol* 4:626–631.
11. Romero S, et al. (2004) Formin is a processive motor that requires profilin to accelerate actin assembly and associated ATP hydrolysis. *Cell* 119:419–429.
12. Xu Y, et al. (2004) Crystal structures of a Formin Homology-2 domain reveal a tethered dimer architecture. *Cell* 116:711–723.
13. Gard DL, Becker BE, Josh Romney S (2004) MAPping the eukaryotic tree of life: Structure, function, and evolution of the MAP215/Dis1 family of microtubule-associated proteins. *Int Rev Cytol* 239:179–272.
14. Brouhard GJ, et al. (2008) XMAP215 is a processive microtubule polymerase. *Cell* 132:79–88.
15. Al-Bassam J, Larsen NA, Hyman AA, Harrison SC (2007) Crystal structure of a TOG domain: Conserved features of XMAP215/Dis1-family TOG domains and implications for tubulin binding. *Structure* 15:355–362.
16. Popov AV, et al. (2001) XMAP215 regulates microtubule dynamics through two distinct domains. *EMBO J* 20:397–410.
17. Wang PJ, Huffaker TC (1997) Stu2p: A microtubule-binding protein that is an essential component of the yeast spindle pole body. *J Cell Biol* 139:1271–1280.
18. van Breugel M, Drechsel D, Hyman A (2003) Stu2p, the budding yeast member of the conserved Dis1/XMAP215 family of microtubule-associated proteins is a plus end-binding microtubule destabilizer. *J Cell Biol* 161:359–369.
19. Slep K, Vale R (2007) Structural basis of microtubule plus end tracking by XMAP215, CLIP-170, and EB1. *Mol Cell* 27:976–991.
20. Bellanger JM, Gonczy P (2003) TAC-1 and ZYG-9 form a complex that promotes microtubule assembly in *C. elegans* embryos. *Curr Biol* 13:1488–1498.
21. Al-Bassam J, van Breugel M, Harrison SC, Hyman A (2006) Stu2p binds tubulin and undergoes an open-to-closed conformational change. *J Cell Biol* 172:1009–1022.
22. Ovechkina Y, Wagenbach M, Wordeman L (2002) K-loop insertion restores microtubule depolymerizing activity of a "neckless" MCAK mutant. *J Cell Biol* 557–562.
23. Okada Y, Hirokawa N (1999) A processive single-headed motor: Kinesin superfamily protein KIF1A. *Science* 283:1152–1157.
24. Spittle C, Charrasse S, Larroque C, Cassimeris L (2000) The interaction of TOGp with microtubules and tubulin. *J Biol Chem* 275:20748–20753.
25. Nakaseko Y, Nabeshima K, Kinoshita K, Yanagida M (1996) Dissection of fission yeast microtubule associating protein p93Dis1: Regions implicated in regulated localization and microtubule interaction. *Genes Cells* 1:633–644.
26. Pollard TD (1986) Rate constants for the reactions of ATP- and ADP-actin with the ends of actin filaments. *J Cell Biol* 103:2747–2754.
27. Segel IH (1975) *Enzyme Kinetics: Behavior and Analysis of Rapid Equilibrium and Steady-State Enzyme Systems* (Wiley, New York).
28. Kerssemakers JW, et al. (2006) Assembly dynamics of microtubules at molecular resolution. *Nature* 442:709–712.
29. Cassimeris L, Gard D, Tran PT, Erickson HP (2001) XMAP215 is a long thin molecule that does not increase microtubule stiffness. *J Cell Sci* 3025–3033.
30. Ciferri C, et al. (2008) Implications for kinetochore-microtubule attachment from the structure of an engineered Ndc80 complex. *Cell* 133:427–439.
31. Wasilko DJ, et al. (2009) The titerless infected-cells preservation and scale-up (TIPS) method for large-scale production of NO-sensitive human soluble guanylate cyclase (sGC) from insect cells infected with recombinant baculovirus. *Protein Expres Purif* 65:122–132.
32. Ashford AJ, Anderson SSL, Hyman AA (1998) *Preparation of Tubulin from Bovine Brain* (Academic, San Diego) p 8.
33. Hyman A, et al. (1991) Preparation of modified tubulins. *Methods Enzymol* 196:478–485.
34. Gell C, et al. (2010) Microtubule dynamics reconstituted in vitro and imaged by single-molecule fluorescence microscopy. *Methods Cell Biol* 95:221–245.
35. Helenius J, Brouhard G, Kalaidzidis Y, Diez S, Howard J (2006) The depolymerizing kinesin MCAK uses lattice diffusion to rapidly target microtubule ends. *Nature* 441:115–119.